NASA CR-112309

Observability of High Altitude Atmospheric Scattering Layers

Derek M. Cunnold*

Massachusetts Institute of Technology

and Charles Stark Draper Laboratory

Cambridge, Massachusetts

Research sponsored by NASA contract - NAS 1-9984

Index category: Unmanned Earth Satellite Systems;

Atmospheric, Space, and Oceanographic Sciences

*Research Associate, MIT Aeronomy Program, C.S. Draper Laboratory,

and Department of Meteorology

This is a revision of AIAA paper 71-1110.

Abstract

The observability of high altitude aerosol and atmospheric scattering layers by a satellite-mounted optical detector is considered. In particular the detectability of a 50 km layer with a wide-angle receiver is investigated. It is found that a layer possessing an optical depth greater than approximately 2×10^{-4} at 3000 Å (i.e. strong enough to affect BUV measurements of ozone) should be detectable with such an instrument provided that the system can be constructed so as to be sensitive to a signal of only 10^{-4} of the sunlight directly incident on the instrument. However it is concluded that a narrow field-of-view satellite-mounted telescope used to scan the earth's horizon has a more general applicability for the detection of high altitude aerosol layers.

Introduction

The particular atmospheric scattering layer calculations to be described in this paper were the result of an attempt to establish the observability of aerosols under various geometrical conditions. These calculations were initiated after Monitor of Ultraviolet Solar Energy (MUSE)[1] observations indicated the presence of anomalous signal enhancements (at approximately 2800 Å) in the solar observations made from the Nimbus 4 satellite. At this wavelength, considerable absorption by atmospheric ozone occurs; therefore, if an atmospheric scattering layer is to be a significant source of energy, it must be located above approximately 40 km. Evidence for the existence of aerosol layers at such high altitudes has tended to be inconclusive becouse of the small amplitude of the scattering that such layers would produce. However we suggest [2] that there is now sufficient observational evidence [3, 4, 5, 6, 7, 8] to believe that an aerosol layer in the region of 50 km exists in the atmosphere--atleast on isolated occasions and at particular locations. It has been suggested [2,9] that such a layer can affect the measurement of atmospheric ozone concentration profiles by the backscattered ultraviolet (BUV) technique in which nadir satellite observations of backscattered radiance at ultraviolet wavelengths are made[10, 11, 12] and it was thus concluded that the BUV technique requires that simultaneous determinations of the aerosol extinction function profile be made.

Both the BUV experiment and the MUSE experiment are on the Nimbus 4 satellite. We have therefore investigated the "anomalous" signal enhancements

that an aerosol layer at 50 km would produce in the MUSE type of observations for which a wide-angle detector was used. The resulting signal enhancements are found to be of small amplitude and this implies that to observe the layer such an instrument must undergo considerable modification. However rather than modify the present instrument it is suggested that a narrow-field-of-view telescope be used for observing the global distribution of high altitude aerosol layers.

Analysis

The geometry of the aerosol scattering problem is illustrated in figure 1. (see the appendix for a list of the symbols used). We assume that the sensitivity and orientation of the detectors is such that the satellite-mounted instrument always views the earth's horizon and is sensitive to radiation within a 45° half-angle cone as in the MUSE instrument. It is further supposed in this analysis that the optical axis of the instrument is located in the plane containing the sun and the local vertical through the satellite. This is the plane in which figure 1 is presented. In the absence of any atmospheric-absorption effects, any scattering from a high-altitude layer (located at height h_a) would be difficult to separate from the Rayleigh scattering and albedo from the lower atmosphere. By working at 3000 Å, however, the lower atmosphere is effectively shielded by atmospheric ozone, and little energy penetrates below 40 km. The ozone absorption cross-section data used in the calculations is taken from Vigroux[15].

Consider the scattering produced by a thin atmospheric layer of forward scatterers which are uniformly distributed over the surface of a sphere of radius $R_o + h_a$. In the absence of absorption, the scattering layer produces a signal enhancement which peaks at the solar-occultation angle for the satellite (which for a satellite altitude of 1100 km is approximately 60°). The shape of the enhancement as a function of angle is similar to the shape of the phase function of the scatterers. However, the surface of the earth will prevent the illumination of those scatterers situated on the night side of the earth. For this reason, the maximum enhancement will, in fact, occur for angles, θ_s, slightly greater than the

solar-occultation angle.

At the wavelengths of interest (~3000 Å), atmospheric ozone is a powerful absorber. Ozone, therefore, plays an important role in determining the signal enhancement, unless the layer of scatterers is situated at a much higher altitude (≥80 km) than the ozone layer. Since the path length of solar radiation through the ozone layer increases rapidly as the satellite angle, θ_s, tends to the solar-occultation angle , atmospheric ozone tends to reduce the enhancement in the neighborhood of the solar-occultation angle. It is thus possible for the enhancement to peak at virtually any angle between the day terminator and the satellite-occultation angle, and the actual location will depend upon the height of the scattering layer and its scattering properties. This suggests the possibility that observations of the scattered energy can yield information on the characteristics of the scattering layer.

For computation purposes we can consider a vertical profile of aerosols to consist of a collection of layers, each of 6 km (for example) depth. A similar computational approach is used for treating the molecular scatterers in the atmosphere. Since particular concern in this paper is directed at an aerosol layer at 50 km, let us consider the scattering produced by a single (6 km) layer of aerosols. We consider only single scattering by the aerosols and assume them to be nonabsorbent. The variation of the ozone concentration over the (vertical) depth of an individual layer is ignored by assuming that the layer is of infinitesimal thickness, located at a particular altitude and uniformly distributed horizontally, and has an optical depth given by

$$S_a = \int_{\substack{\text{layer} \\ \text{depth}}} \sigma_a \rho_a(h_a) dh_a \qquad (1)$$

where σ_a is a mean scattering depth cross-section for the aerosols and $\rho_a(h_a)$ is the concentration of the scatterers.

Little information is available a present on the scattering properties of the 50 km aerosol layer. We have therefore calculated aerosol phase functions for spherical particles based upon certain assumed aerosol size distributions. The calculations assumed that the concentration of aerosols (n) with radii between r and r + dr could be related to their size by the usual expression

$$n(r) = A\, r^{-\alpha}\, dr \qquad (2)$$

where A is a constant related to the total density of aerosols and α is a parameter which may be prescribed. For the well-known aerosol layer at approximately 20 km, values of α between 2 and 4 are commonly used[13, 14], while for the 50 km layer Elliott[7] has suggested an $\alpha = 7$. Figure 2 contains plots of the phase functions calculated for values of α of 3 and 7 at 3000 Å, assuming spherical non-absorbent particles with a refractive index of 1.5*. The calculated wavelength dependence of aerosol extinction for these two values of α is depicted in figure 2. It may

*Particle size cut-offs of 0.04μ and 2μ were assumed in this calculation. The results for $\alpha = 7$ tend to be sensitive to the size used for the lower cut-off limit. The lower limit of 0.04μ was chosen only because it is a value that is often used in stratospheric aerosol calculations.

be noted that the dependence is weaker than that for molecular scatterers. Figure 2 also contains plots of the expression

$$a(\chi) = \frac{1 + \chi_o^{-2}}{2\pi(1 + e^{-\pi/\chi_o})} e^{-|\chi|/\chi_o} \qquad (3)$$

where χ is the phase angle, for $\chi_o = 0.25$ and 0.04. It may be noted that the mean of the latter curves is a reasonable approximation to the phase function for $\alpha = 3$. In the succeeding calculations, for mathematical simplicity, we have arbitrarily assumed that the aerosol phase function may be represented by expression (3) and we have investigated the limb enhancements for $\chi_o = 0.04$, 0.1, and 0.25.

The pattern function of the receiver/detector is simply assumed to be given by

$$P = 1 \quad \text{if} \quad |\chi| < \theta_s - \frac{\pi}{4}$$
$$= 0 \quad \text{if} \quad |\chi| \geq \theta_s - \frac{\pi}{4}$$

This representation of the response of the wide-angle receiver is considered to be adequate for purposes of this study. The ozone concentration profile used in the calculations is based upon the limited number of rocket observations which are available at the present time[16, 17].

The contribution of the aerosol layer to the scattered energy is given as an integral over the surface located at height h_a. The integration in the azimuthal (ϕ) direction is evaluated approximately so that the surface integral is expressed as $2\phi_o$ times the scattered contribution

for $\phi = 0$. The surface integral is thus reduced to an integral over θ_a which is then evaluated numerically. ϕ_o is defined by the ray from the detector which is tangential to the sphere of radius $R_o + h_a$ and which meets the sphere at (θ_a, ϕ_o) - unless a smaller real value of ϕ_o is given by the angle at which the phase function declines to 1/e of its value at $\phi = 0$.

Results for an Isolated Scattering Layer

Examples of the scattered contribution at several wavelengths produced by a layer of atmospheric scatterers localised in height but uniformly distributed horizontally and located at several different altitudes are given in Figures 4 - 7. Figure 4 depicts the effect of varying the layer height. At the wavelength of 3000 Å for a layer height greater than about 80 km, the effect of atmospheric absorption is small. It may be noted that for $\chi_o = 0.25$ the peak scattered intensity can be somewhat greater than the value S_a times the solar intensity. The effect of atmospheric ozone is to reduce the intensity of the scattered radiation at most of the angles shown, but particularly for those satellite angles in the vicinity of the solar-occultation angle. Figures 5 and 6 contain results for various values of χ_o. Figure 5 demonstrates that in the absence of absorption effects, the shape of the enhancement produced by scattering is similar to the shape of the phase function and is centered about the solar-occultation angle. This result is produced in Figure 5 because, for very strong forward scatterers, the effect of atmospheric abserption is relatively constant over the small angle range of interest. The peak intensity is found to be very much larger for the strongest forward scatterers, because a layer with a small vertical optical depth can produce substantial scattering, because the optical depth in the viewing direction is roughly two orders of magnitude larger than in the vertical

Figure 6 shows that as the phase function of the scatterers

becomes more sharply peaked the location of the maximum scattered signal tends to increase and to move closer to the solar occultation angle. However for a layer at 45 km ozone absorption becomes dominant for $\chi_o > 0.25$ so that the peak scattered signal is in fact determined by $\chi_o \sim 0.25$.

Figure 7 shows the effect of wavelength on enhancement. This variation is produced by the wavelength dependence of the ozone absorption coefficient. The results are similar to those produced by varying the layer height. For shorter wavelengths (corresponding to more ozone absorption), the maximum of the enhancement moves closer to the day terminator, and the maximum enhancement diminishes. A similar result is obtained by reducing the height of the scattering layer (see Figure 4).

Figures 4-7 indicate that <u>if the contribution from a layer of atmospheric scatterers can be isolated</u>, information about the height of such a layer and its scattering properties may be obtained with a wide angle receiver and filters sensitive to several ultraviolet wavelengths.

Total Atmospheric Scattering

In the previous section we considered the scattering produced by an isolated layer of aerosols having $S_a = 10^{-3}$. This optical depth is produced by a layer of approximately 6 km width having an extinction roughly equal to that for molecular scatterers at 50 km and at 3000 Å. The observations of the 50 km aerosol layer on the other hand have been made at visible wavelengths and they suggest an extinction comparable with that for molecular scatterers at the wavelengths used and at that height. Since little information is available on the scattering properties of these aerosols, it is not possible to infer the aerosol extinction at ultraviolet wavelengths, although an extinction of the same order of magnitude as that due to molecular scatterers at 50 km may be regarded as an upper bound for the aerosol extinction. On the other hand, it has been estimated[2] that if aerosols are to affect BUV measurements of ozone, the extinction at 50 km and 2800 Å must be greater than 10% of that for molecular scatterers. Clearly molecular scattering may thus adversely affect the detectability of the aerosols of interest since the extinction for molecular scatterers is comparable with that of the aerosols.

To illustrate the observability of this aerosol layer we have arbitrarily assumed an extinction equal to 1.25 times that for Rayleigh scatterers at 50 km and 3000 Å. The aerosol phase function used is the mean of those given by expression (3) with $\chi_o = 0.25$ and 0.04. As has already been mentioned this phase function model is regarded as an adequate approximation to $\alpha = 3$ aerosols (which aerosols appear to be typical of the 20 km stratospheric aerosol layer). The contribution from molecular

scattering has been computed using a phase function defined by expression (3) with $\chi_o = 2.0$. The various contributions and the total scattered signal at 3000 Å and 2800 Å are shown in Figures 8 and 9. It is to be noted that the aerosols produce a considerable enhancement of the scattered energy at satellite locations beyond the day terminator ($\theta_s = 90°$). At 2800 Å, considerably more of the forward scattered energy (mainly produced by the aerosols) is removed by ozone absorption, as compared to the results for 3000 Å.

Figures (8) and (9) further suggest that an aerosol layer at 50 km having an extinction comparable with that for molecular scatterers at 3000 Å should be detectable with a wide angle receiver. The figures suggest a detectability limit with such an instrument of order 0.2 that for extinction by molecular scatterers. It is particularly to be noted however that the scattered signal is only 0.1% of the directly incident solar energy. Thus, to detect aerosols capable of affecting BUV observations, a detector of the type considered would have to be sensitive to fluctuations of approximately 10^{-4} against the background of directly incident solar energy, and the instrument would have to possess baffling sufficient to prevent signals of this amplitude and scattered by the instrument housing from entering the detector. The MUSE instrument does not possess this capability and is therefore incapable of detecting a 50 km aerosol layer with an extinction which is less that or equal to that from molecular scatterers at 50 km and 3000 Å. These considerations in fact imply a degree of sophistication if a wide angle detection system is to be used for monitoring such high altitude aerosol layers. Since a coronograph is specifically designed to prevent directly incident solar energy from entering a detector it could form the basis of such a wide angle instrument.

A Limb-Scanning Telescope

We have considered whether the MUSE type of instrument might be modified to detect the 50 km aerosol layer, and for detecting other high altitude aerosol layers. A wide angle instrument possesses the limitation that it must be operated at approximately 3000 Å so that, by virtue of absorption by ozone, the energy scattered by an aerosol layer may be separated from that produced by molecular scatterers in the lower atmosphere. However, it is reasonable to expect that the wavelength dependence of aerosol scattering is weaker, and could in fact be considerably weaker, than that for molecular scatterers. Thus, if the scattering from 50 km, for example, can be isolated, high altitude aerosol layers (including the BUV related layer) would be more easily detected by making measurements at visible wavelengths (e.g., 5000-7000 Å). A narrow-field-of-view telescope may be used for this purpose.

A wide angle detection system also permits only one average atmospheric scattering layer to be derived per orbit while a horizon-scanning telescope allows many observations per orbit. A limb-scanning telescope therefore has wider applicability to the detection of high-altitude aerosol layers than a wide-angle MUSE-type instrument. Such a satellite-mounted telescope used to scan the earth's horizon with an altitude resolution of 1 km should yield the extinctions and scattering properties of stratospheric aerosols as a function of both altitude and wavelength[8, 16]. An example of a simulated limb scan with such a device in the presence of a 50 km aerosol layer having an extinction equal to that for molecular scatterers at that height and at 3000 Å is shown in Figure 10. At a solar zenith angle of 69° (i.e., a scattering angle of 21°) the layer produces a signal enhancement comparable with the signal resulting from molecular scattering.

Conclusions

The detectability of an aerosol layer with a wide-angle satellite-mounted detector has been discussed. Information about its height and scattering properties may be obtained by monitoring the energy at several ultraviolet wavelengths as a function of satellite location. However, the detectability of this layer strongly depends upon its scattering properties about which little is known at the present time. A layer possessing an optical depth greater than approximately 2×10^{-4} at 3000 Å (i.e., strong enough to affect BUV measurements of ozone) should be detectable with a wide-angle instrument provided that the observing system can be constructed so as to be sensitive ot a signal of only 10^{-4} of the sunlight directly incident on the instrument. However, it is concluded that the 50 km aerosol layer is not detectable with the MUSE instrument. For systematically monitoring the global distribution of high altitude aerosol layers, a wide-angle instrument possesses certain limitations and it was suggested that a narrow-field-of-view telescope which scans the earth's horizon be used.

References

[1]Nimbus Project, The Numbus IV User's Guide, National Space Science Data Center, Goddard Space Flight Center, Greenbelt, Maryland, 1970, pp. 135-148.

[2]Cunnold, D.M., Gray, C.R., and Merritt, D.C., "Stratospheric aerosol layer detection," Journal of Geophysical Research, Vol. 78, 1973, pp. 920-931.

[3]Meinel, M.P., and Meinel, A.B., "Late twilight golw of the ash stratum from the eruption of Agung volcano," Science, Vol. 142, November 1963, pp. 582-583.

[4]Mateer, C.L., "Twilight colors seen from space," NCAR Quarterly, Vol. 20, August 1968.

[5]Rossler, F., "The aerosol layer in the stratosphere," Space Research, Vol. 8, 1968, North Holland Publishing Co., Amsterdam, pp. 633-636.

[6]Clemesha, B.R., and Nakamura, Y., "Dust in the upper atmosphere," Nature, Vol. 237, February 1972, pp. 328-329.

[7]Elliott, D.D., "Effects of a high altitude (50 km) aerosol layer on topside ozone sounding," Space Research, Vol. 11, 1971, Akademie-Verlag, Berlin, pp. 857-861.

[8]Gray, C.R., Malchow, H.L., Merritt, D.C., and Var, R.E., "Aerosol monitoring by satellite horizon scanning, Journal of Spacecraft and Rockets, Vol. 10, 1973, pp. 71-76.

[9]Cunnold, D.M., Gray, C.R., and Merritt, D.C., "Aerosols: A limitation on the determination of ozone from BUV observations, Pure and Applied Geophysics, Vol. 106-108, 1973, pp. 1264-1271.

[10]Sekera, Z., and Dave, J.V., Comments made at the Symposium on Atmospheric Ozone, Arosa, Seiterland, August 14-19, 1961, Published in International Union of Geodesy and Geophysics Monograph No. 19, 1962.

[11]Twomey, S., and Howell, H.B., "A discussion of indirect sounding methods with special reference to the deduction of vertical ozone distribution from light scattering measurements," Monthly Weather Review, Vol. 91, No. 4, 1963, pp. 659-664.

[12]Anderson, G.P., Barth, C.A., Cayla, F., and London, J., "Satellite observations of the vertical ozone distribution in the upper stratosphere," Annals de Geophysique, Vol. 25, No. 1, 1969, pp. 341-345.

[13]Newkirk, G., and Eddy, J.A., "Light scattering by particles in the upper atmosphere," Journal of the Atmospheric Sciences, Vol. 21, January 1964, pp. 35-60.

[14]Rosen, J.M., "Stratospheric dust and its relationship to the meteoritic flux," Space Science Reviews, Vol. 9, No. 1, 1969, pp. 58-89.

[15]Vigroux, E., "Contributions a l'etude experimentale de l'absorption de l'ozone," Annales de Physique, Vol. 8, Serie 12, 1953, pp. 709-762.

[16]Newell, R.E., and Gray, C.R., "Meteorological and ecological monitoring of the stratosphere and mesosphere," Final report of M.I.T. Aeronomy Project, NASA CR-2094, August, 1972.

[17]Krueger, A.J., "Stratospheric ozone distribution from 24 rocket soundings; mean and extreme values between 60°S and 64°N," Pure and Applied Geophysics, 106-108, 1973, pp. 1272-1280.

Appendix

List of Symbols

θ_s is the angular location of the satellite with $\theta_s = 0$ being the antisolar direction

θ_a, ϕ is the angular location of an element of the aerosol scattering layer in polar coordinates with the polar axis being the antisolar direction

$\phi_o(\theta_a)$ is an azimuthal angle of an element of the scattering layer; in the calculations scattered contributions from $\phi > \phi_o$ are neglected.

h_a is the altitude of the aerosol layer

S_a is the (vertical) optical depth of the aerosol layer

R_o is the radius of the earth

χ is the angle between the direction opposite to the satellite motion and a line drawn between the detector and the element of the scattering layer.

χ_o is a parameter used in the mathematical representation of the aerosol phase function. It is approximately the value of χ at which the phase function falls to 1/e of its value at $\chi = 0$.

α is an index used to represent the distribution of particle sizes within the aerosol layer.

λ is the wavelength (Angstroms) at which observations are assumed to be made

Figure Captions

Figure 1: The geometry of the scattering-layer satellite detector problem. The aerosol layer at height h_a is situated in the atmospheric ozone layer and is viewed at angle χ relative to the optic axis with a fixed wide angle detector located on the satellite.

Figure 2: Aerosol phase functions for size distributions represented by $\alpha = 3$ and 7. Also shown are two model phase functions used in the computations and defined by expression (3) with $\chi_o = 0.04$ and 0.25.

Figure 3: A comparison of the wavelength dependence of aerosol extinction for size distributions represented by $\alpha = 3$ and 7. The aerosols were assumed to be non-absorbent with refractive index 1.5 and a lower cut-off size of .04μ was assumed. The extinctions were normalized to be equal at 5577 Å.

Figure 4: Examples of the scattering produced by an aerosol layer located at heights of 50, 60, and 80 km. The wavelength was 3000 Å and the phase function was assumed to be given by expression (3) with $\chi_o = 0.25$.

Figure 5: Examples of the scattering produced at 3000 Å by an aerosol layer located at 60 km altitude. Curves are plotted for aerosol phase functions given by expression (3) with $\chi_o = 0.25$, 0.1, and 0.04.

Figure 6: Examples of the scattering produced at 3000 Å by an aerosol layer located at 45 km altitude. Curves are plotted for aerosol phase functions given by expression (3) with $\chi_o = \pi$, 0.25, and 0.1.

Figure 7: Examples of the scattering produced at 2800, 2900, and 3000 Å by an aerosol layer located at 50 km altitude. The aerosol phase function was assumed to be given by expression (3) with $\chi_o = 0.25$.

Figure 8: The total scattering (sum) produced in a realistic atmosphere at 3000 Å by an aerosol layer located at 50 km altitude. The aerosol phase function was assumed to be given by the mean value of expression (3) with $\chi_o = 0.25$ and 0.04. The contribution from Rayleigh scattering was modeled with a phase function given by $\chi_o = 2.0$.

Figure 9: The total scattering (sum) produced in a realistic atmsophere at 2800 Å by an aerosol layer located at 50 km altitude. The aerosol and Rayleigh phase functions were similar to those described in the caption to Figure 8.

Figure 10: A 3000 Å limb scan of the atmosphere containing an aerosol layer located at 50 km. The aerosol phase function was that given in Figure 2 with $\alpha = 3$ and the scattering angle was approximately 21°. The abscissa refers to the altitude at which the line drawn through the axis of the instrument is closest to the surface of the earth (i.e., tangent height).

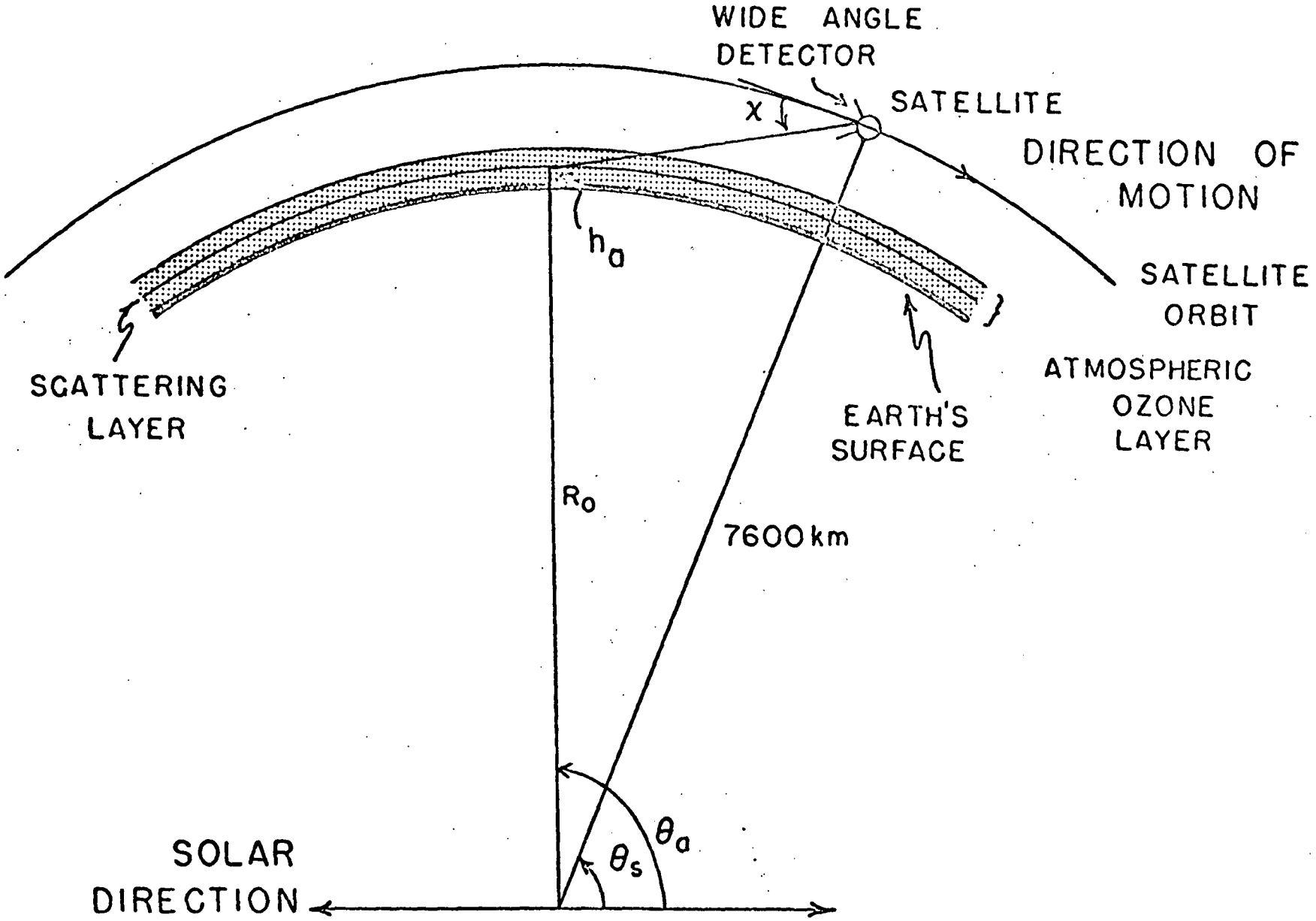
WIDE ANGLE
DETECTOR
SATELLITE
χ
DIRECTION OF
MOTION
h_a
SATELLITE
ORBIT
SCATTERING
LAYER
EARTH'S
SURFACE
ATMOSPHERIC
OZONE
LAYER
R_o
7600 km
θ_a
θ_s
SOLAR
DIRECTION

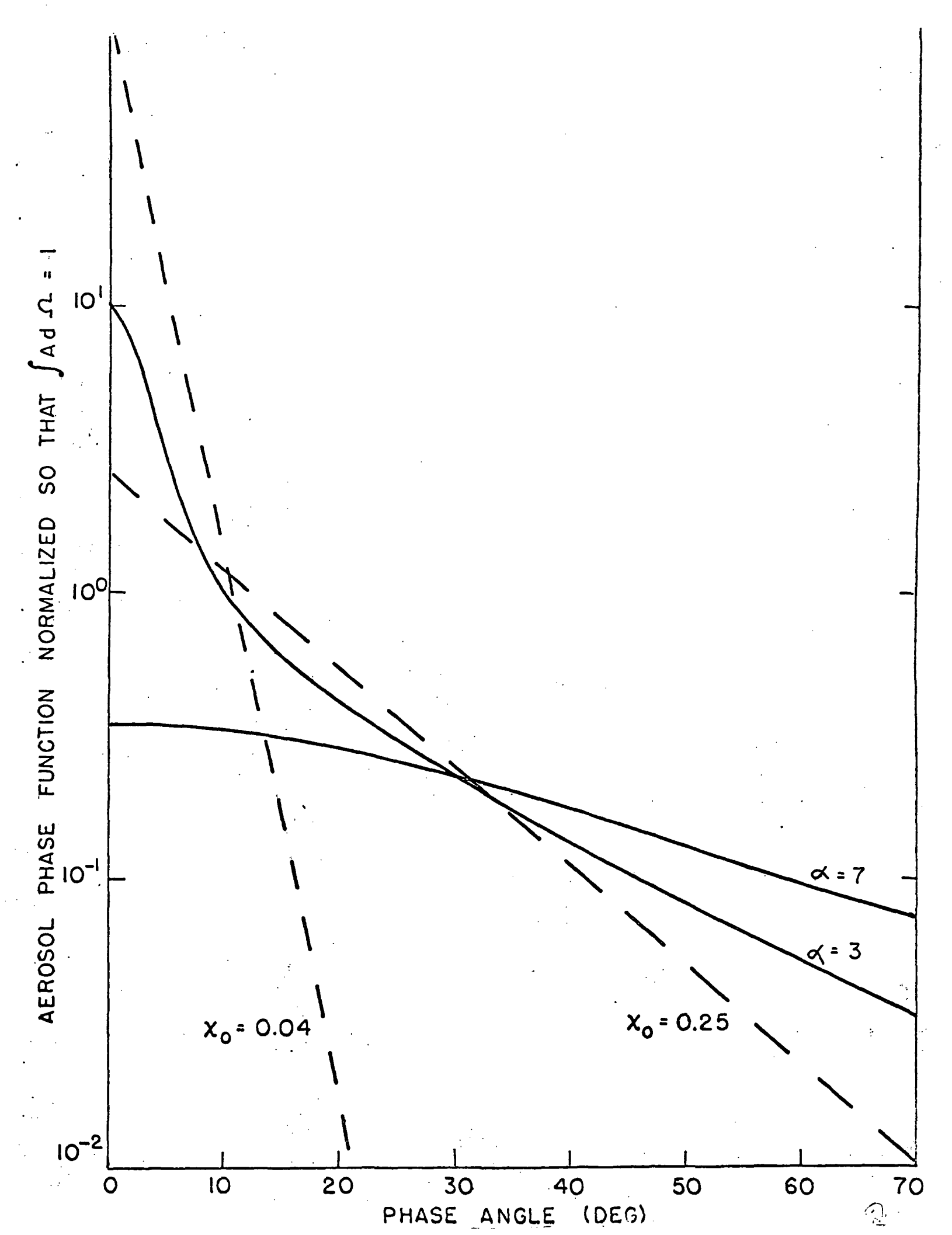
AEROSOL PHASE FUNCTION NORMALIZED SO THAT $\int A\, d\Omega = 1$
10^{1}
10^{0}
10^{-1}
10^{-2}
0
10
20
30
40
50
60
70
PHASE ANGLE (DEG)
$\alpha = 7$
$\alpha = 3$
$\chi_0 = 0.04$
$\chi_0 = 0.25$

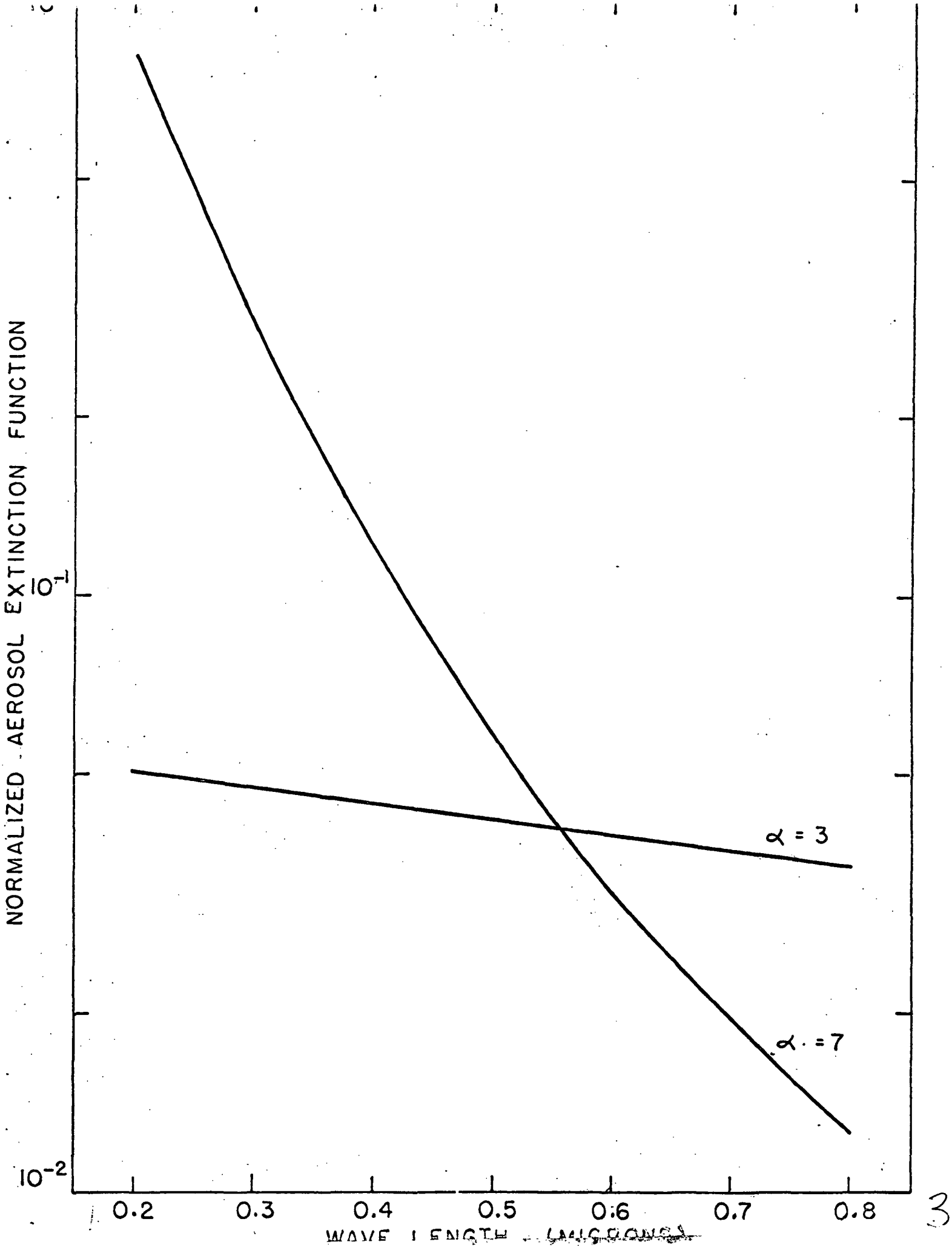
NORMALIZED AEROSOL EXTINCTION FUNCTION
10^{-1}
10^{-2}
$\alpha = 3$
$\alpha = 7$
0.2
0.3
0.4
0.5
0.6
0.7
0.8
WAVE LENGTH - (MICRONS)

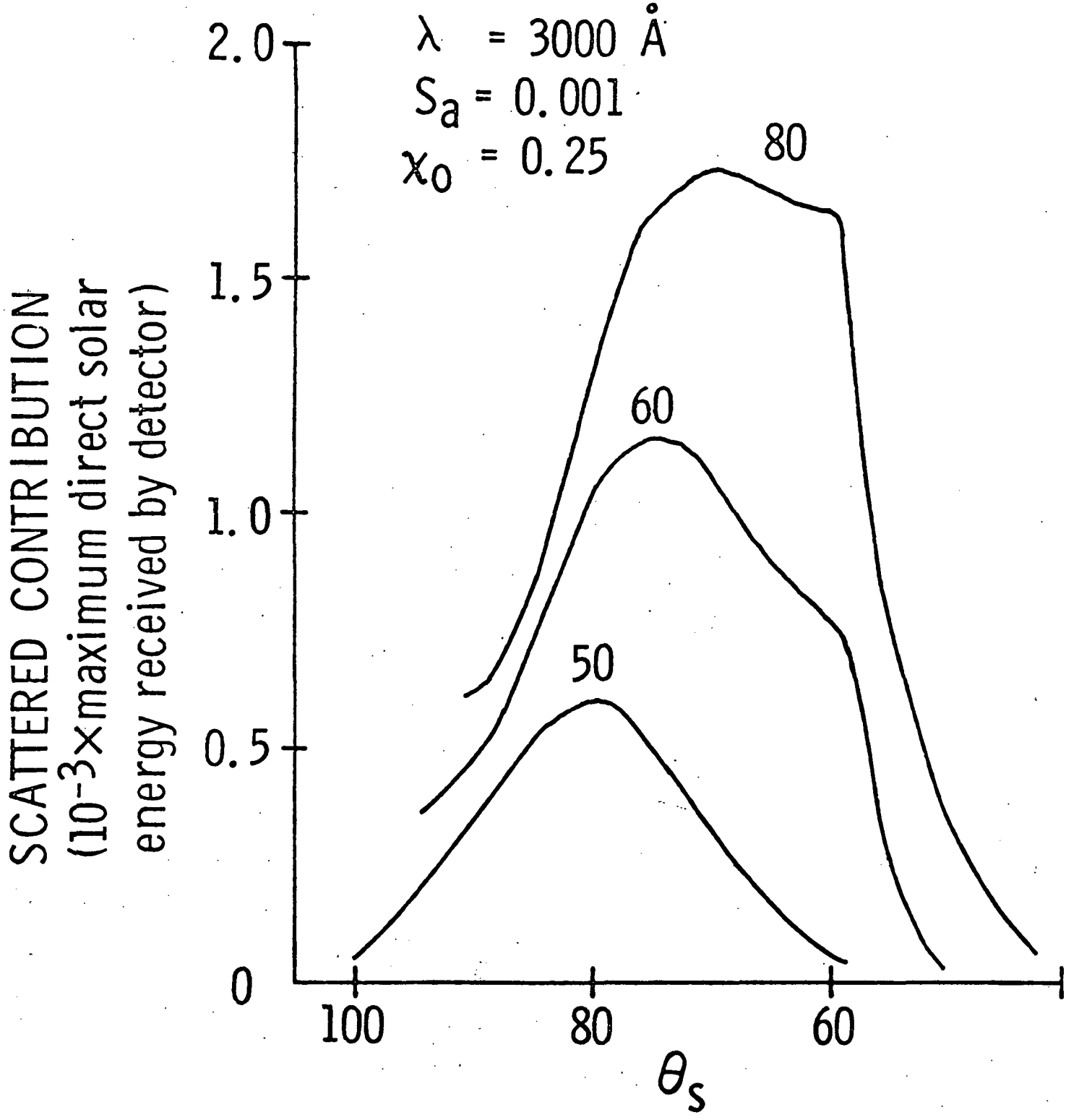
λ = 3000 Å
S_a = 0.001
χ_o = 0.25
SCATTERED CONTRIBUTION
(10⁻³×maximum direct solar
energy received by detector)
2.0
1.5
1.0
0.5
0
80
60
50
100
80
60
θ_s

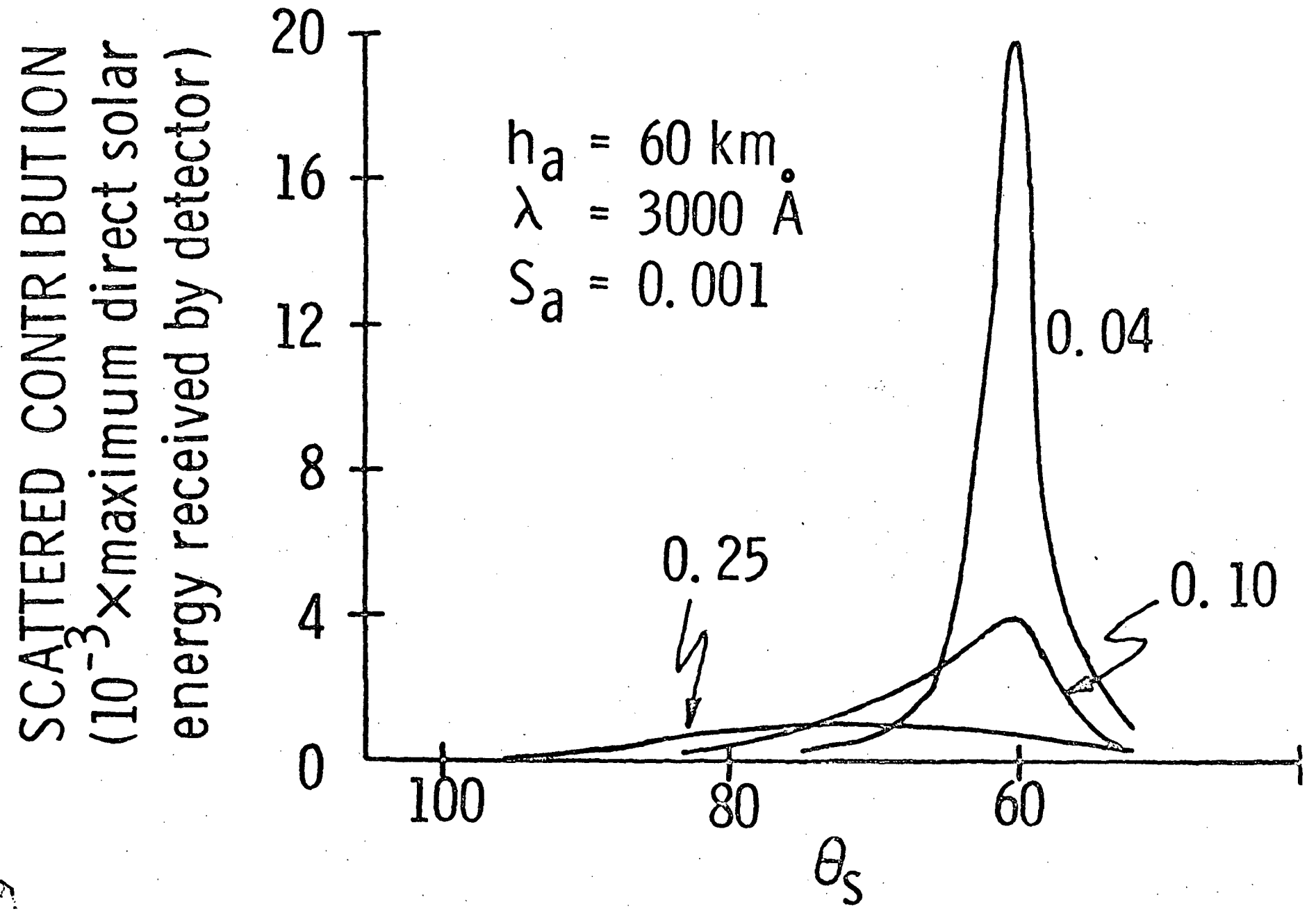
SCATTERED CONTRIBUTION
(10^{-3} × maximum direct solar
energy received by detector)
20
16
12
8
4
0
h_a = 60 km
λ = 3000 Å
S_a = 0.001
0.04
0.25
0.10
100
80
60
θ_s

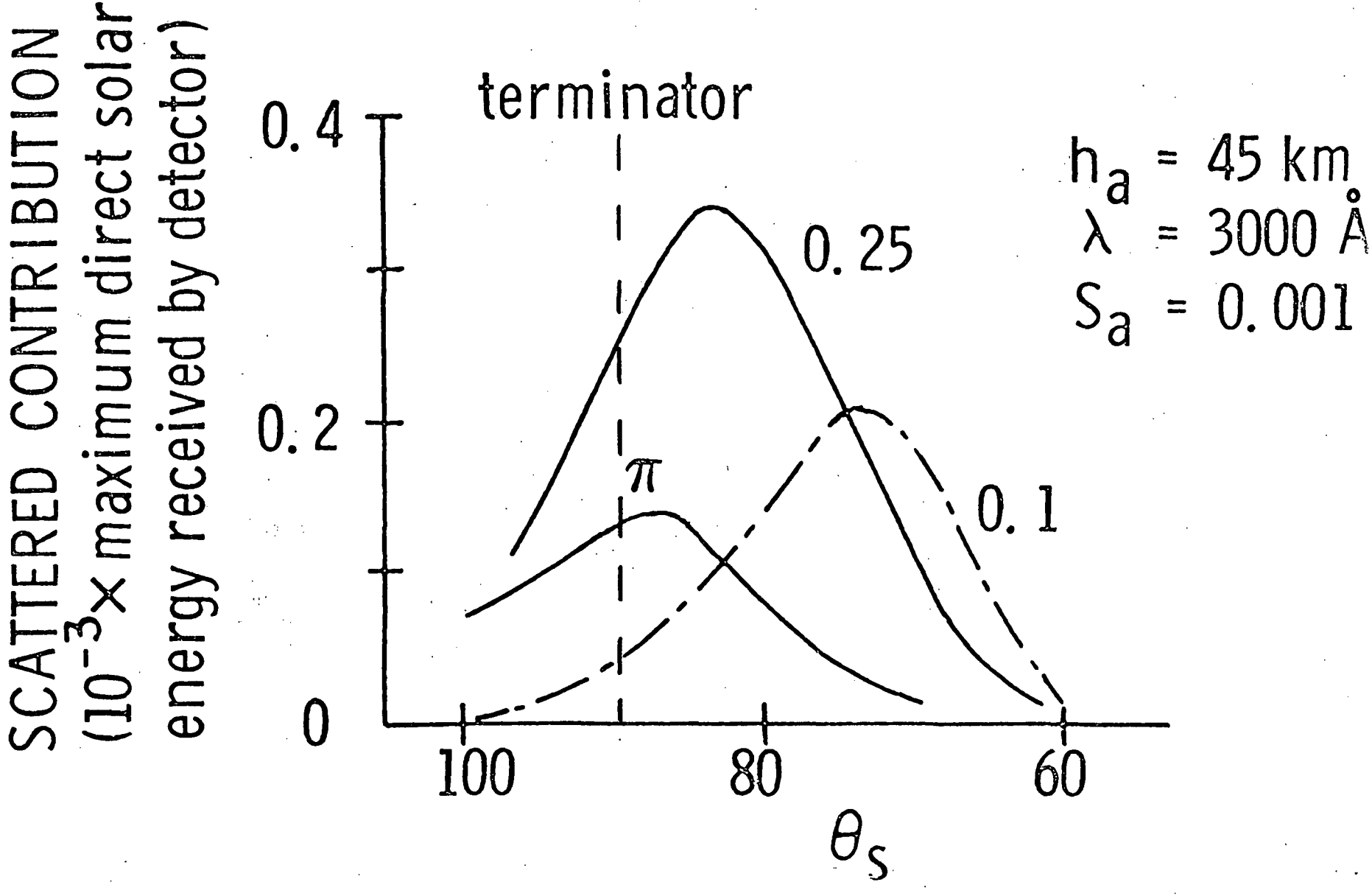
SCATTERED CONTRIBUTION
(10^{-3} × maximum direct solar
energy received by detector)
terminator
0.4
0.2
0
0.25
0.1
π
h_a = 45 km
λ = 3000 Å
S_a = 0.001
100
80
60
θ_s

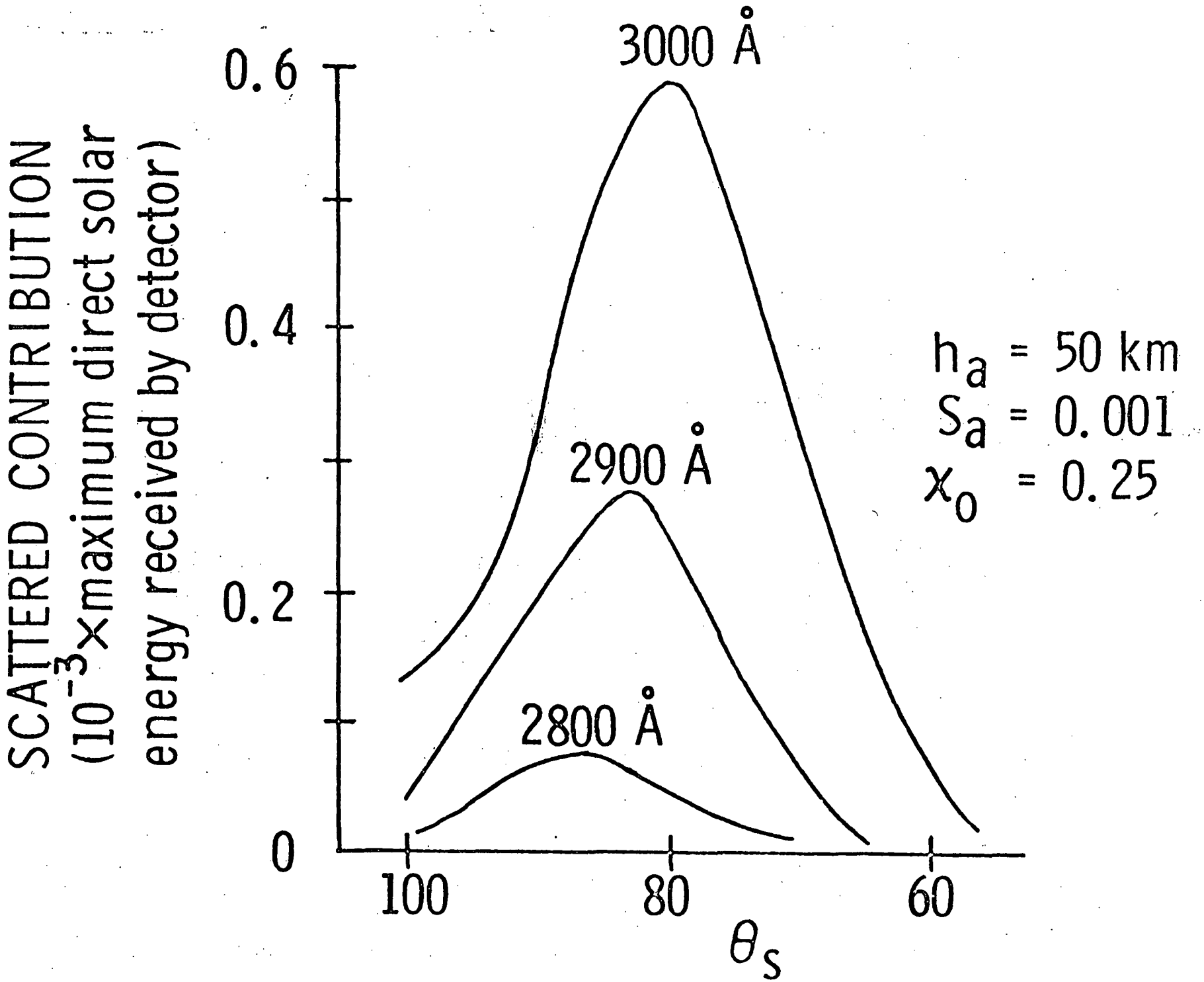
SCATTERED CONTRIBUTION
(10^{-3} × maximum direct solar
energy received by detector)
0.6
0.4
0.2
0
3000 Å
2900 Å
2800 Å
h_a = 50 km
S_a = 0.001
χ_0 = 0.25
100
80
60
θ_s

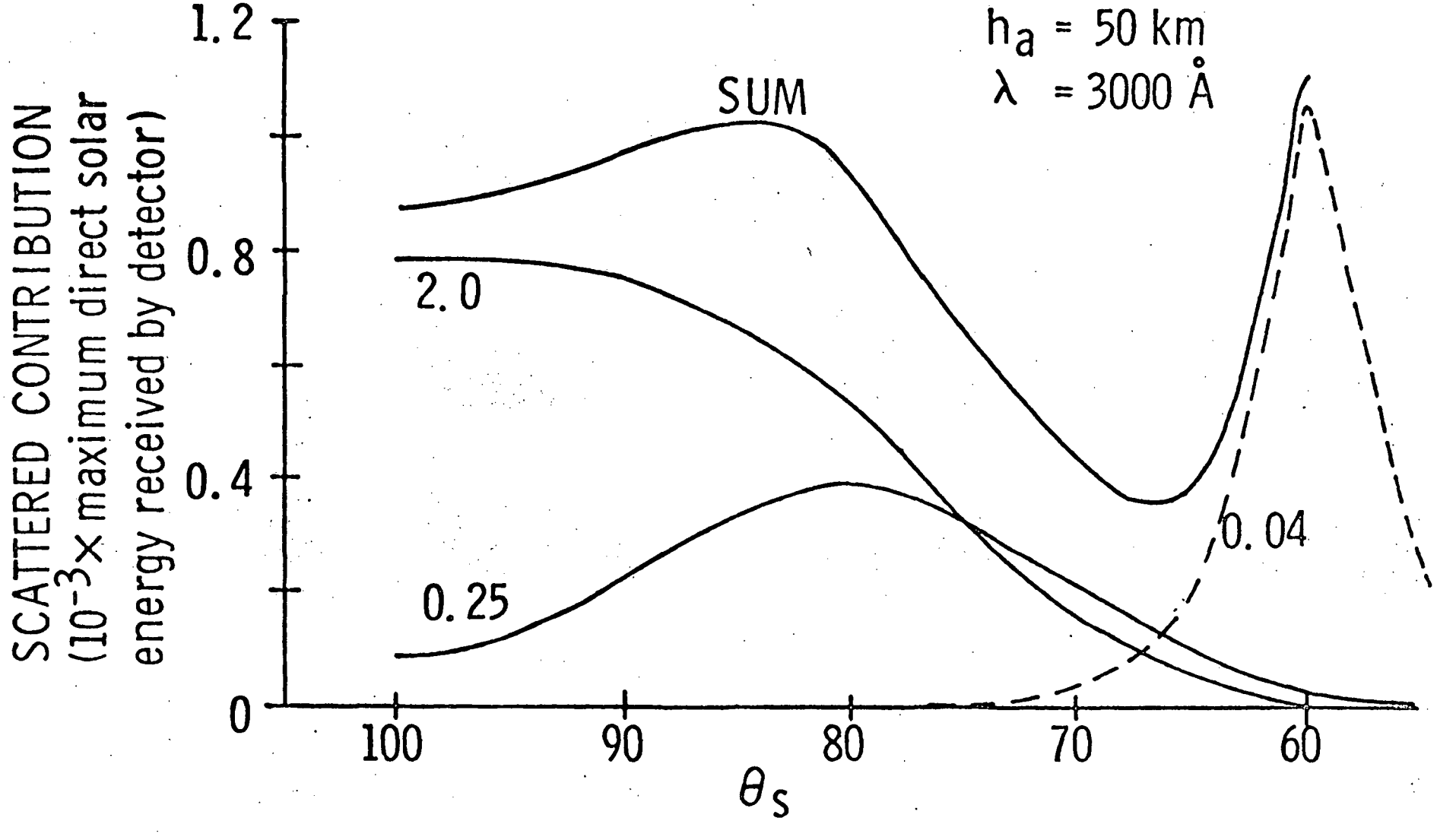
SCATTERED CONTRIBUTION
(10^{-3} × maximum direct solar energy received by detector)
1.2
0.8
0.4
0
100
90
80
70
60
θ_s
h_a = 50 km
λ = 3000 Å
SUM
2.0
0.25
0.04

SCATTERED CONTRIBUTION
(10^{-3} × maximum direct solar
energy received by detector)
0.4
0.2
0
100
90
80
70
60
θ_s
h_a = 50 km
λ = 2800 Å
SUM
2.0
0.25

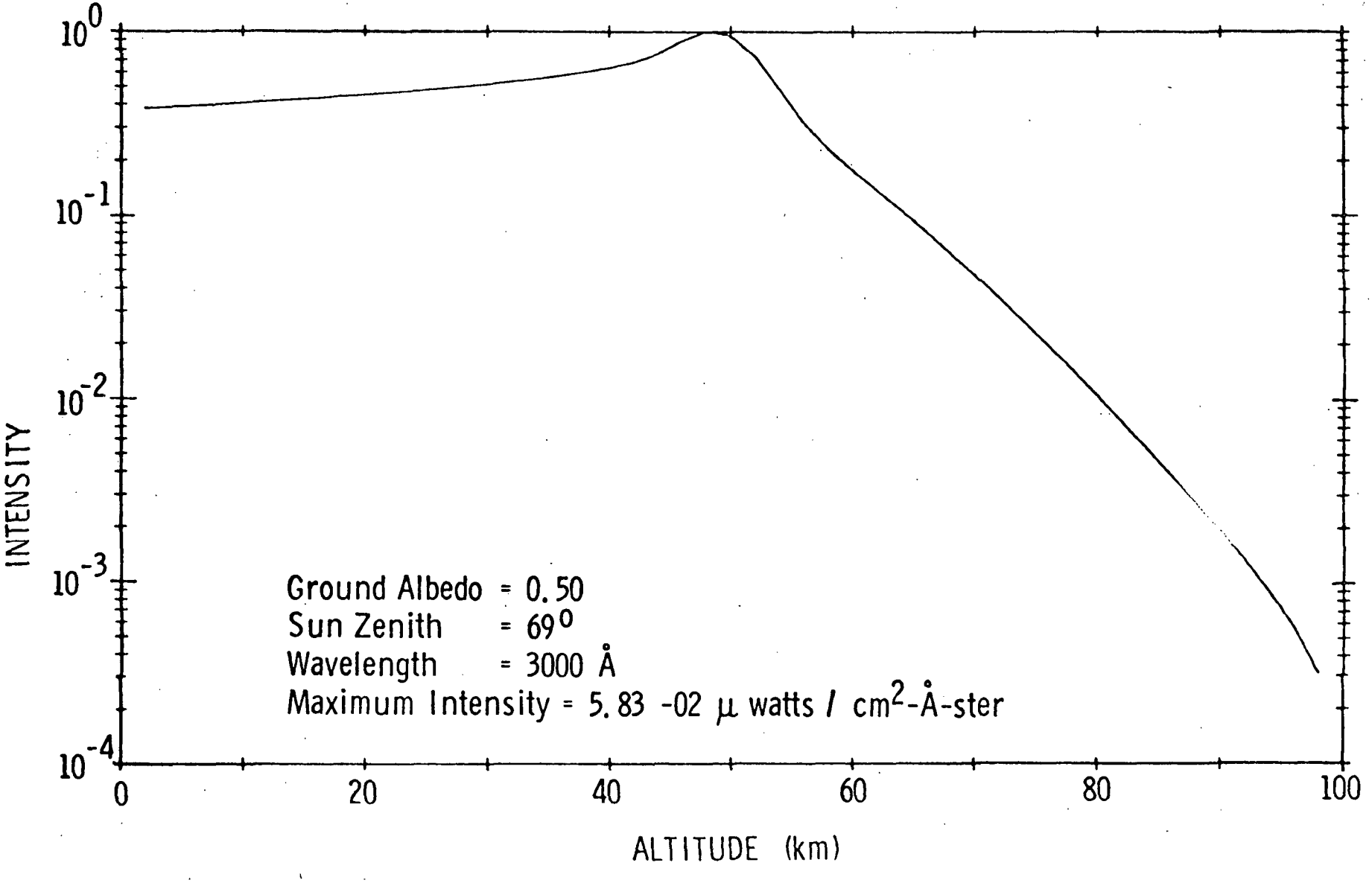
INTENSITY
10^{0}
10^{-1}
10^{-2}
10^{-3}
10^{-4}
0
20
40
60
80
100
ALTITUDE (km)
Ground Albedo = 0.50
Sun Zenith = 69°
Wavelength = 3000 Å
Maximum Intensity = 5.83 -02 μ watts / cm²-Å-ster